Multiobjective Collaborative Beamforming for a Distributed Satellite Cluster via NSGA-II

Bo Xi[1,2], Tao Hong[1,2(✉)], and Gengxin Zhang[1,2]

[1] National Engineering Research Center, Nanjing University of Posts and Telecommunications, Nanjing 210003, China
hongt@njupt.edu.cn

[2] Key Lab of Broadband Wireless Communication and Sensor Network Technology, Ministry of Education, Nanjing University of Posts and Telecommunications, Nanjing 210003, China

Abstract. In this paper, a distributed satellite cooperative beamforming algorithm is proposed for the satellite cluster formed by multiple distributed formation flying satellites in the space information network. The average pattern function of distributed formation satellites is derived based on random antenna array theory. On this basis, a multiobjective optimization is formulated to enhance the transmit signal in the desired direction while suppress the interference in the undesired direction via nondominated sorting genetic algorithm II (NSGA-II). The simulation results show that the proposed method extends the distributed and cooperative beamforming technology to the research field of space information network and enhances the electromagnetic wave transceiver capability of resource-constrained satellite systems.

Keywords: Space information network · Distributed satellite cluster · Collaborative beamforming · Random arrays · NSGA-II

1 Introduction

Satellite communication has become one of the key technologies in 5G mobile communication network to meet the requirement of the global coverage [1]. Compared with the wireless link of the terrestrial cellular system, the satellite link has the characteristics of large attenuation because of the long distance transmission. Furthermore, the total power of a satellite transponder and antenna aperture is limited due to the satellite launch cost. It is difficult to improve the transmission performance and channel capacity of a satellite link. Therefore, how to improve the electromagnetic wave transceiver capability of resource-constrained satellite systems has become a hot research topic in the field of space information network [2].

Distributed and collaborative beamforming (DCBF) technique is proposed in wireless sensor networks (WSNs) to enhance the transmission performance of the sensor nodes [3]. The solid initial works on the random antenna array paved way to the statistical analysis of collaborative beamforming was presented by Ochiai et al. [4]. On this basis, Ahmedin in [5] investigated the performances of DCBF when the location information of sensor nodes follows the uniformly and Gaussian probability density

J. Zheng et al. (Eds.): ADHOCNETS 2019, LNICST 306, pp. 252–261, 2019.
https://doi.org/10.1007/978-3-030-37262-0_21

function (pdf), and summarized the advantage of 3 dB mainlobe width with uniformly pdf and sidelobe performance with Gaussian pdf, respectively. However, these results based on a particular pdf for a WSNs may not be true for the practical WSNs model. In [6], Huang proposed a novel unified method based on non-parametric kernel to evaluate DCBF performance for various node distributions. In [7], Buchanan extended the WSNs model from 2-dimensional model to 3-dimensional motion-dynamic model, such as unpiloted air vehicle (UAV) clusters scenario.

Compared with the sensor nodes with random distribution characteristic in a certain area, the location information of the distributed formation flying satellites in a space information network has two properties: one is the orbit-project location information with fixed characteristic; the other is the perturbation information, caused by non-spherical of earth, light pressure, lunisolar gravitational and so on, with random distribution characteristic. Thus, the fixed and random characteristics are co-existence for the location information of a distributed formation flying satellites. To enhance the electromagnetic wave transceiver capability of a distributed formation flying satellites, we proposed a cooperative beamforming algorithm to fit the location information characteristic of a distributed formation flying satellites. We derive the average far-field beampattern based on random antenna array theory. Furthermore, a multiobjective optimization is formulated to enhance the transmit signal in the desired direction while suppress the interference in the undesired direction via nondominated sorting genetic algorithm II (NSGA-II) Simulation results showed that the proposed method can obtain a optimal formation of a distributed formation flying satellites for a fixed electromagnetic wave transceiver task.

2 Average Beampattern of the Proposed Collaborative Beamforming

The system model for a distributed formation flying cluster with N satellites is shown in Fig. 1. The fixed location information for nth satellite is $P_n(r_n, \theta_n, \phi_n)$, where $\theta_n \in [0, \pi]$ and $\phi_n \in [0, 2\pi)$. We assume that the instantaneous actual location information $P'_n(r'_n, \theta'_n, \phi'_n)$, off of the fixed location information caused by the satellite perturbation, for nth satellite is random located in a spherical volume of radius B. The desired direction is denoted by $P_0(r, \theta_0, \phi_0)$.

The following practical considerations and mathematical assumptions arise in this context: (1) the synchronization amongst satellites is assumed sufficient for high-fidelity phase control or time delay with negligible degradation from frequency offsets or phase jitter, (2) all satellites have equal power and all signals experience equal path losses, and (3) the channels between satellites and the target are all ideal. Thus, there are no multipath fading and shadowing.

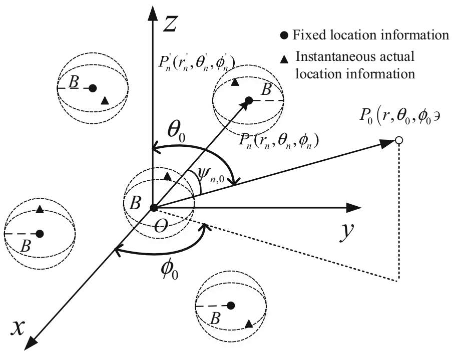

Fig. 1. System model for a distributed formation flying cluster

According to the system model in Fig. 1, the manifold vector is written as:

$$\begin{aligned} A_n(\theta,\phi) &= \overbrace{e^{j\cdot\frac{2\pi}{\lambda}r_n'\left(\cos\psi_n' - cos\psi_{n,0}'\right)}}^{\text{random term}} \cdot \overbrace{e^{j\cdot\frac{2\pi}{\lambda}r_n\cos\psi_n}}^{\text{fixed term}} \\ &= e^{j\cdot\frac{2\pi}{\lambda}\left[r_n'\left(\cos\psi_n' - cos\psi_{n,0}'\right) + r_n\cos\psi_n\right]}, n = 1,2,\cdots,N \end{aligned} \tag{1}$$

where:

$$\cos\psi_n = \sin\theta\sin\theta_n\cos(\phi-\phi_n) + \cos\theta\cos\theta_n \tag{2a}$$

$$\cos\psi_n' = \sin\theta\sin\theta_n'\cos\left(\phi-\phi_n'\right) + \cos\theta\cos\theta_n' \tag{2b}$$

$$\cos\psi_{n,0}' = \sin\theta_0\sin\theta_n'\cos\left(\phi_0-\phi_n'\right) + \cos\theta_0\cos\theta_n' \tag{2c}$$

for the sake of analysis the manifold vector $A_n(\theta,\phi)$, we define the following variables as:

$$\rho_0 = \sqrt{(\sin\theta\cos\phi - \sin\theta_0\cos\phi_0)^2 + (\sin\theta\sin\phi - \sin\theta_0\sin\phi_0)^2} \tag{3a}$$

$$\cos\delta = \rho_0^{-1}(\sin\theta\cos\phi - \sin\theta_0\cos\phi_0) \tag{3b}$$

$$\sin\delta = \rho_0^{-1}(\sin\theta\sin\phi - \sin\theta_0\sin\phi_0) \tag{3c}$$

$$\delta = \tan^{-1}\left[\frac{\sin\theta\sin\phi - \sin\theta_0\sin\phi_0}{\sin\theta\cos\phi - \sin\theta_0\cos\phi_0}\right] \tag{3d}$$

$$\cos\gamma = \rho_0^{-1}(\cos\theta - \cos\theta_0) \tag{3e}$$

Substitute (3) into (1), the manifold vector can be also presented as follows:

$$A_n(\theta,\phi) = e^{j\cdot\frac{2\pi}{\lambda}\left\{r_n'\rho_0\left[\sin\theta_n'\cos\left(\phi_n'-\delta\right) + \cos\theta_n'\cos\gamma\right] + r_n\cos\psi_n\right\}} \tag{4}$$

We also define the following variables simplify the express as:

$$I_n = R_n\sin\theta_n'\cos\left(\phi_n'-\delta\right), -1 \le I_n \le 1 \tag{5a}$$

$$Q(\theta,\phi) = 2\pi\beta\rho_0 \tag{5b}$$

$$T_n = R_n\cos\theta_n', -1 \le T_n \le 1 \tag{6a}$$

$$G(\theta) = 2\pi\beta\rho_0\cos\gamma \tag{6b}$$

$$L_n = \frac{r_n}{\lambda} \tag{7}$$

where $R_n = r_n'/B$, $\beta = B/\lambda$ denotes the normalizated perturbation radius, L_n is the normalizated distance between the nth satellite and the center of coordinate system. Substitute (5)–(7) into (4), we obtain as follows:

$$A_n(\theta,\phi) = e^{j\cdot\{[I_nQ(\theta,\phi) + T_nG(\theta)] + 2\pi L_n\cos\psi_n\}} \tag{8}$$

To obtain the statistical average of the manifold vector $A_n(\theta,\phi)$, we introduce a variable $U_n(-1 \le U_n \le 1)$, satisfied with $U_n^2 + I_n^2 + T_n^2 \le 1$. Without loss of generality, we consider the instantaneous actual location information with the uniformly pdf represented by $f_{r',\phi',\theta'}$ (for the practical perturbation model, the pdf can be obtained by the proposed algorithm in [7]). Therefore, we can derive the pdf for (r',θ',ϕ') as follows:

$$\int_0^1 f_{r'}r'^2dr' = 1 \rightarrow f_{r'} = 3 \tag{9a}$$

$$\int_0^\pi f_{\theta'}\sin\theta'd\theta' = 1 \rightarrow f_{\theta'} = \frac{1}{2} \tag{9b}$$

$$\int_0^{2\pi} f_{\phi'}d\phi' = 1 \rightarrow f_{\phi'} = \frac{1}{2\pi} \tag{9c}$$

The joint probability density function of U_n, I_n, and T_n satisfies as:

$$\int_0^1\int_0^{2\pi}\int_0^\pi f_{U_n,I_n,T_n}r'^2dr'\sin\theta'd\theta'd\phi' = 1 \rightarrow f_{U_n,I_n,T_n} = \frac{3}{4\pi} \tag{10}$$

The joint probability density function of I_n and T_n satisfies as:

$$f_{I_n,T_n} = \int_{-\sqrt{1-T_n^2-I_n^2}}^{\sqrt{1-T_n^2-I_n^2}} f_{U_n,,I_n,T_n} \mathrm{d}U_n = \frac{3}{2\pi}\sqrt{1-T_n^2-I_n^2} \tag{11}$$

thus, the average manifold vector can be written as:

$$\begin{aligned}\bar{A}_n(\theta,\phi) &= \int_{-1}^{1}\int_{-\sqrt{1-I_n^2}}^{\sqrt{1-I_n^2}} A_n(\theta,\phi) f_{I_n,T_n} \mathrm{d}T_n \mathrm{d}I_n \\ &= 6tinc(Q(\theta,\phi))jinc(G(\theta))\mathrm{e}^{j\cdot 2\pi L_n(\sin\theta\sin\theta_n\cos(\phi-\phi_n)+cos\theta\cos\theta_n)}\end{aligned} \tag{12}$$

where $tinc(x) = J_1(x)/x$, $jinc(x) = j_1(x)/x$, $J_1(x)$ denotes the first spherical Bessel function of the first order, and $j_1(x)$ denotes the first Bessel function of the first order. Without loss of generality, we consider the direction $(\theta_0,\phi_0) = \left(90^{\circ}, 0^{\circ}\right)$ as the desired direction and the beampattern in azimuth plane $(\theta = 90^{\circ})$ in the following sections. Thus, the variables Q and G satisfied with $Q(\theta,\phi) = 4\pi\beta\sin(\phi/2)$ and $G(\theta) = 0$. Thus, the average manifold vector can be rewritten as:

$$\bar{A}_n(\phi) = 3tinc(\alpha(\phi))\mathrm{e}^{j\cdot 2\pi L_n\sin\theta_n\cos(\phi-\phi_n)} \tag{13}$$

where $\alpha(\phi) = 4\pi\beta\sin(\phi/2)$. The average beampattern is presented as:

$$F(\phi) = \frac{1}{N}\sum_{n=1}^{N} 3tinc(\alpha(\phi))\mathrm{e}^{j\cdot 2\pi L_n\sin\theta_n\cos(\phi-\phi_n)} \cdot w_n \tag{14}$$

where $w_n \in C$ denotes the weighted value for nth satellite, C denotes the complex field, and $\boldsymbol{w} = [w_1, w_2, \cdots, w_n]^{\mathrm{T}}$ is the weighted vector for the array. The average power pattern can be written as:

$$S(\phi) = |F(\phi)|^2 = \frac{1}{N^2}|\sum_{n=1}^{N} 3tinc(\alpha(\phi))\mathrm{e}^{j\cdot 2\pi L_n\sin\theta_n\cos(\phi-\phi_n)} \cdot w_n|^2 \tag{15}$$

We also define the following variables simplify the express as:

$$K(\phi) = \left||F_s(\phi)|^2 - |F(\phi)|^2\right| = \frac{1}{N^2}\left|\left|\sum_{n=1}^{N} w_n \cdot A_n(\phi)\right|^2 - \left|\sum_{n=1}^{N} w_n \cdot \bar{A}_n(\phi)\right|^2\right| \tag{16}$$

similar to the peak-to-average ratio of OFDM signal, we use the complementary cumulative distribution function (CCDF) to evaluate this beampattern difference as:

$$C_{K(\phi)}(z) = P(K(\phi) > z) = 1 - P(K(\phi) \le z) \tag{17}$$

3 Optimization Algorithm Design

The NSGA-II algorithm is based on Pareto theory. The multi-objective optimization problem is related to the fast sorting of non-dominated solution sets, which makes the population approach the Pareto front quickly. At the same time, it introduces the Crowding degree coefficient, and abandons the artificially designated parameters of the shared radius in the previous generation algorithm, which better guarantees the diversity of the population. At the same time, an elite strategy was introduced to prevent the loss of the superior solution [8].

Algorithm Framework of the Optimization

Initially generating the initial population of N individuals
Define the largest evolutionary algebra *MaxGen*;
While $gen < MaxGen$ **do**
  For $i = 1$ to N **do**
    Fast non-dominated sorting:
    Calculate three objective function values according to formula (18);
    the same layer of individuals have the same non-dominated sorting(i_{rank});
    Crowding degree coefficient:
    Sort by f_1, f_2, f_3;
    Marginal individual = ∞;
    $i_d = \sum_{j=0}^{3}(|f_j^{i+1} - f_j^{i-1}|)$
    Preserve quality individuals:
    If $i_{rank} < j_{rank}$ **or** $i_{rank} = j_{rank}$ **and** $i_d > j_d$
      Preserve i;
    End
  End
  Crossover, mutation, generate the next generation population;
End

4 Simulation Results

Faced with complex spatial network environments, it is necessary to generate corresponding null in strong signal interference sources. Under the condition of $N = 10$, $\beta = 15, L_n = 303$, the desired direction is $\phi_0 = 0°$, and the undesired direction interval is: $\phi \in [0.3°, 0.32°]$, which is intended to produce null in this interval. At the same time, the peak sidelobe level (PSL) is also suppressed to eliminate complex signal interference in the spatial network. The independent variables are: the elevation angle of the nth satellite: $\theta_n \in [0, \pi]$, the azimuth angle of the nth satellite: $\phi_n \in [0, 2\pi)$, and the weight phase $\alpha_n \in [-\pi, \pi]$, and the optimization target is established according to the scene requirements. The function is described by a mathematical formula as:

$$\begin{cases} \min\limits_{\phi_n,\theta_n,\alpha_n} & f_1 = 20\log_{10}|F_{av}(\phi_{ML})| \\ \min\limits_{\phi_n,\theta_n,\alpha_n} & f_2 = 20\log_{10}\left|\frac{\max|F_{av}(\phi_{SL})|}{F_{av}(\phi_{ML})}\right| \\ \min\limits_{\phi_n,\theta_n,\alpha_n} & f_3 = 20\log_{10}\left|\frac{\max|F_{av}(\phi_k)|}{F_{av}(\phi_{ML})}\right|, \phi_k \in [0.3°,0.32°] \\ s.t. & w_n^H w_n = 1, \quad n = 1,2,\ldots,N \end{cases} \tag{18}$$

where ϕ_{SL} is the angle of the sidelobe during the optimization process, and ϕ_{ML} is the angle of the mainlobe. $\phi_k \in [0.3°, 0.32°]$ is the null of the beampattern.

Figure 2 shows that the relationship between mainlobe and PSL/null. We can get better PSL or null by properly sacrificing the performance of the mainlobe.

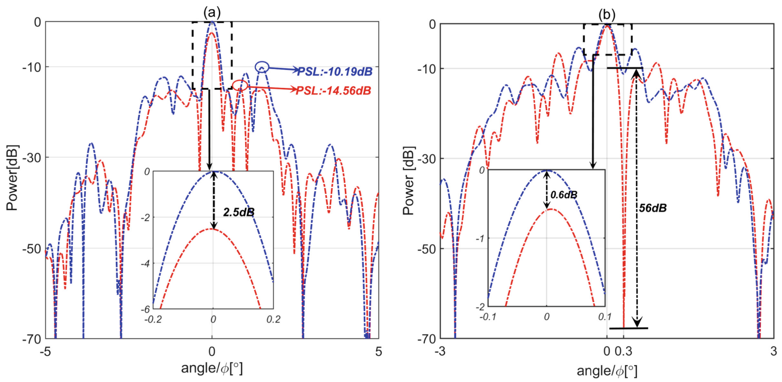

Fig. 2. (a) Relationship between mainlobe and PSL (b) Relationship between mainlobe and null

Figure 3 shows that when the mainlobe power tends to the maximum value, the PSL is also gradually increased. Furthermore, it is a pair of nonlinear contradictory parameters, and we can use this property according to the specific task requirements.

Through the formation of Fig. 4 we can get the beampattern shown in Fig. 5, the desired source azimuth angle: 0°, the maximum power of the array is obtained. The strong signal interference source: (0.3°, 0.32°) forms a null, which can reach about −40 dB. At the same time, the PSL is controlled at −9 dB, which meets the needs of the task.

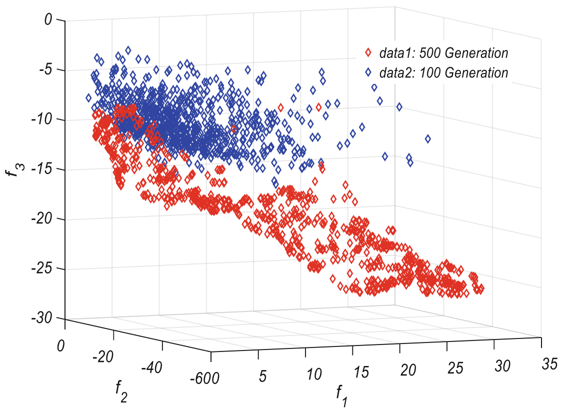

Fig. 3. Pareto frontier solution cluster

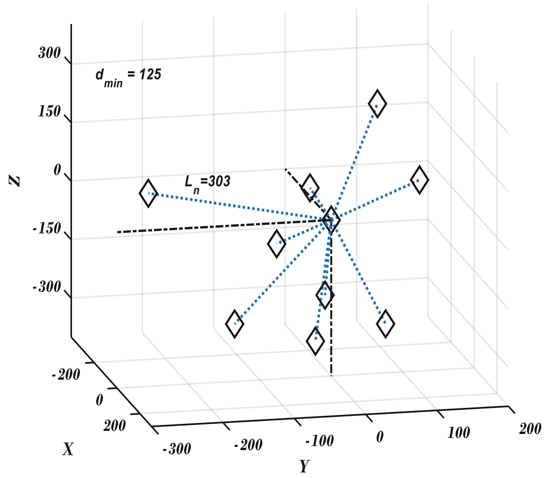

Fig. 4. Satellite cluster formation

The CCDF shows the probability that the average power pattern approaches the instantaneous beampattern. It can be seen that as the threshold power increases, the probability decreases continuously, and the probability of the average power pattern jitter of 4 dB is less than 1%.

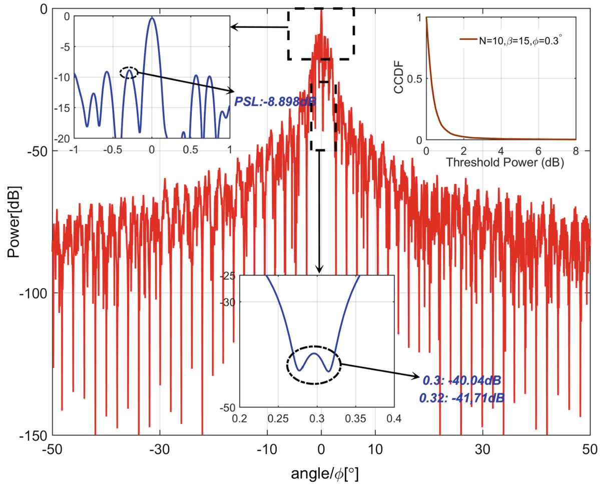

Fig. 5. Array power pattern

5 Conclusion

In this paper, a distributed satellite cooperative beamforming algorithm for the satellite cluster formed by multiple distributed formation flying satellites in space information network is proposed to enhance the electromagnetic wave transceiver capability of a resource-constrained satellite system. Simulation results show that the proposed method extends the distributed and cooperative beamforming technology to the research field of space information network. The issues to be studied in the future such as adaptive beamforming algorithm in high dynamic environment, optimal formation for a electromagnetic wave transceiver task, synchronized methods of a distributed satellites formation flying and so on.

Achnowledgement. The work presented in this paper is partially supported by the National Science Foundation of China (No. 91738201, No. 61801445, No. 61971440). However, any opinion, finding, and conclusions or recommendations expressed in this material; are those of the author and do not necessarily reflect the views of the National Science Foundation.

References

1. Boero, L., Bruschi, R., Davoli, F.: Satellite networking integration in the 5G ecosystem: research trends and open challenges. IEEE Netw. **32**(5), 9–15 (2018)
2. Yu, Q.Y., Meng, W.X., Yang, M.C.: Virtual multi-beamforming for distributed satellite clusters in space information networks. IEEE Wirel. Commun. **23**(1), 95–101 (2016)
3. Jayaprakasam, S., Rahim, S.K.A., Leow, C.Y.: Distributed and collaborative beamforming in wireless sensor networks: classifications, trends and research directions. IEEE Commun. Surv. Tutorials. **19**(4), 2092–2116 (2017)

4. Ochiai, H., Mitran, P., Poor, H.V.: Collaborative beamforming for distributed wireless ad hoc sensor networks. IEEE Trans. Signal Process. **53**(11), 4110–4124 (2005)
5. Ahmed, M.F.A., Vorobyov, S.A.: Collaborative beamforming for wireless sensor networks with gaussian distributed sensor nodes. IEEE Trans. Wirel. Commun. **8**(2), 638–643 (2009)
6. Huang, J., Wang, P., Wan, Q.: Collaborative beamforming for wireless sensor networks with arbitrary distributed sensors. IEEE Commun. Lett. **16**(7), 1118–1120 (2012)
7. Buchanan, K., Huff, G.H.: A stochastic mathematical framework for the analysis of spherically-bound random arrays. IEEE Trans. Antennas Propag. **62**(6), 3002–3011 (2014)
8. Deb, K., Pratap, A., Agarwal, S.: A fast and elitist multiobjective genetic algorithm: NSGA-II. IEEE Trans. Evol. Comput. **6**(2), 1–197 (2002)